Multimodal study of Default-Mode Network integrity in Disorders of Consciousness

Cristina Rosazza[1,2] PhD, Adrian Andronache[1] PhD, Davide Sattin[3] Psy D, Maria Grazia Bruzzone[1] MD, Giorgio Marotta[6] MD, Anna Nigri[1] MSc, Stefania Ferraro[1] MSc, Davide Rossi Sebastiano[4] MD, Luca Porcu[7], Anna Bersano[5] MD, Riccardo Benti[6] MD, Matilde Leonardi[3] MD, Ludovico D'Incerti[1]* MD, Ludovico Minati[2]* PhD CEng CPhys CSci, on behalf of the Coma Research Centre (CRC) – Besta Institute

[1]Neuroradiology Unit, [2]Scientific Department, [3]Neurology, Public Health, Disability Unit, [4]Department of Neurophysiology-Epilepsy Center, [5]Cerebrovascular Disease Unit, Fondazione IRCCS Istituto Neurologico "Carlo Besta", Milano, Italy; [6]Department of Nuclear Medicine, Fondazione IRCCS Ca' Granda Ospedale Maggiore Policlinico, Milano, Italy.

[7] Laboratory of Methodology for Biomedical Research, Oncology Department, IRCCS - Istituto di Ricerche Farmacologiche "Mario Negri", Milano, Italy

*These authors contributed equally

Address correspondence to:

Dr. Cristina Rosazza

Scientific Department and Neuroradiology Dept.

Fondazione IRCCS Istituto Neurologico "Carlo Besta"

Via Celoria 11 20133 Milano Italy

Tel. +39-02-23942449

✉cristina.rosazza@istituto-besta.it

Title: N characters = 80

Word count: Manuscript N words: 6119; Abstract N words = 249; Introduction N words = 606;

Discussion N words = 1961

Running head: DMN integrity in DOC (N characters = 20)

1 Table, 3 Figures, 7 Supplementary Tables

ABSTRACT

Objective: Understanding residual brain function in Disorders of Consciousness poses extraordinary challenges, and imaging examinations are needed to complement clinical assessment. The default-mode network (DMN) is known to be dysfunctional, although correlation with level of consciousness remains controversial. We investigated DMN activity with resting-state functional MRI (rs-fMRI), alongside its structural and metabolic integrity, aiming to elucidate the corresponding associations with clinical assessment.

Methods: We enrolled 119 consecutive patients: 72 vegetative state/unresponsive wakefulness state (VS/UWS), 36 minimally-conscious state (MCS) and 11 severe disability. All underwent structural MRI and rs-fMRI, and a subset also performed FDG-PET. Data were analyzed with manual and automatic approaches, in relation to diagnosis and clinical score.

Results: Excluding the quartile with largest head movement, DMN activity was decreased in VS/UWS compared to MCS, and correlated with clinical score. Independent-component and seed-based analyses provided similar results, though the latter and their combination were most informative. Structural MRI and FDG-PET were less sensitive to head movement and had superior diagnostic accuracy than rs-fMRI only when all cases were included. Rs-fMRI indicated relatively preserved DMN activity in a small subset of VS/UWS patients, two of whom evolved to MCS. The integrity of the left hemisphere appears predictive of a better clinical status.

Interpretation: Rs-fMRI of the DMN is sensitive to clinical severity. The effect is consistent across data analysis approaches, but heavily dependent on head movement. Rs-fMRI could be informative to detect residual DMN activity for those patients that remain relatively still during scanning and whose diagnosis is uncertain.

INTRODUCTION

Disorders of consciousness (DOC) encompass a spectrum of conditions ranging from coma, vegetative state/unresponsive wakefulness state (VS/UWS), minimally conscious state (MCS) to severe disability (SD). Diagnosis, prognosis and planning of rehabilitation in patients with DOC remain challenging.[1] The clinical assessment of residual consciousness at the bedside is difficult particularly between VS/UWS and MCS, and there remain difficulties in determining antemortem the location, type and severity of central nervous system pathology causing DOC in single patients.[2-6]

Neuroimaging methods complement clinical diagnosis and neurophysiological investigations for assessing residual consciousness and cognitive function. MRI is the preferred method to visualize the location and extent of damage to the cortex, midbrain and upper brain stem. Depending on aetiology, structural imaging shows heterogeneous lesion patterns including diffuse axonal injury, multifocal cortical contusions and thalamic damage. The potential of structural MRI in the study of DOC has been less thoroughly investigated, while advanced MRI techniques such as Diffusion Tensor Imaging (DTI) have been used to differentiate VS/UWS from MCS.[7]

Key advances in understanding DOC have come from ^{18}F-fluorodeoxyglucose positron emission tomography (FDG-PET). FDG-PET studies in resting-state conditions demonstrated considerable decrease in brain metabolism in DOC, namely, medial and lateral fronto-parietal associative cortices are the most hypometabolic areas in VS/UWS and have better preserved metabolism in MCS.[2, 8-10] Recent studies have confirmed that metabolic integrity can disentangle VS/UWS from MCS patients with good accuracy and predict clinical outcome.[11,12]

To extend PET findings, functional MRI has been applied in resting-state conditions and during active tasks. Resting-state functional MRI (rs-fMRI) reveals multiple cortical networks of synchronized activity. One of these networks is known as the default-mode network (DMN) which encompasses the precuneus, lateral parietal cortex and mesial prefrontal cortex. It subserves large-scale integrative processes related to mind wandering, memory consolidation and awareness.[13-15] The DMN activity, plausibly alongside all other cortical networks, is absent in brain death and irreversible coma but can be partially preserved in VS/UWS.[18-23] In MCS, the DMN is somewhat stronger than in VS/UWS, but severely impaired compared to healthy subjects.[20,21,23] Recently, it has been shown that preservation of functional connectivity between frontal and parietal DMN regions is a significant marker for recovery from coma after 3 months[24].

While in other domains rs-fMRI is capable of attaining rather high diagnostic accuracy levels,[25-27] its clinical value in DOC remains unclear. Rs-fMRI is highly sensitive to head movement and DMN detection critically depends on data filtering choices.[28] Yet, while active techniques such as mental imagery have very high specificity for conscious awareness, rs-fMRI may deliver increased sensitivity to residual brain activity given that it does not require active patient compliance. To date, only few studies have reported correlation with the clinical signs of consciousness as measured by the CRS-R scale,[20,21] and to our knowledge no study has detected statistically-significant differences in DMN activity between VS/UWS and MCS at the group level. In addition, these findings relate to relatively small patient samples (approximately 14-25 cases), with few exceptions (e.g. Ref. (29) with 53 DOC patients) and generally the patients included were on average in sub-acute phase.[20-23,29]

Here, we investigated the association between DMN integrity and consciousness level represented as diagnosis (VS/UWS, MCS or SD) and clinical assessment (CRS-R scores) in 119 DOC patients

with disease duration on average longer than 2 years. An element of novelty is that DMN integrity was assessed multimodally: *i*) functionally, based on Independent Component Analysis (ICA) and seed-based analysis (SBA) of rs-fMRI, rated both automatically and visually by expert operators; *ii*) anatomically, based on visual ratings of anatomical damage in the DMN regions, as visualized by conventional MRI scans; *iii*) metabolically, based on average FDG uptake measures in the DMN regions.

METHODS

Participants

Adult DOC patients, who underwent a 1-week programme of multidisciplinary assessment between 2011-2013 at the Coma Research Centre (CRC) of the Fondazione IRCCS Istituto Neurologico Carlo Besta, Milan, Italy, were enrolled prospectively. The study was approved by the institutional ethics committee (ref. CRC). Rs-fMRI was performed in 119 of the 153 consecutive DOC patients admitted during the study period; data from all these patients were included in the present analyses. A subgroup of 85 patients also underwent FDG-PET at the Fondazione IRCCS Ca' Granda Ospedale Maggiore Policlinico, Milan, Italy. Demographic and clinical characteristics are reported in Table 1. According to the Aspen criteria,[30] 72 patients were clinically classified as VS/UWS, 36 MCS and 11 SD. Aetiology included 42 anoxic brain injury, 41 vascular brain injury, 36 traumatic brain injury; median disease duration was 26 months (range 2-252), >12 months for 92 cases, and median age was 52 years (range 19-83).

Patients were assessed with the Italian version of the CRS-R;[31,32] each patient was independently assessed 4 times by experienced raters and the best response was used to establish the final value.

A group of 33 healthy participants (median age 39 years, range 17-66) with no history of neurological deficits was recruited as controls.[28] Written informed consent was obtained from patient guardians and healthy participants.

MRI Data Acquisition

Scanning was performed on a 3 T scanner with a 32-channel head coil (Achieva TX, Philips Healthcare BV, Best, NL). The following structural images were acquired: volumetric MP-RAGE T_1-weighted, sagittal T_1-weighted TSE IR, axial T_2-weighted TSE and coronal FLAIR; except for the volumetric series, in-plane resolution was ~0.9 mm with 4 mm slice thickness. For rs-fMRI, 200 GE-EPI volumes were acquired with TR=2.8 s, TE=30 ms, α=70°, 2.5 mm isotropic voxel size, 90×95 matrix size, 50 slices with 10% gap, ascending order. Sequence duration was ~9.5 min. When patient posture allowed, the head was restrained using foam pillows, and a knee wedge was positioned to minimize spine movement and discomfort. Sedation was never performed.

Rs-fMRI Data Preprocessing

A preprocessing pipeline including standard modules implemented in SPM8 (Wellcome Trust Centre for Neuroimaging, London, UK) and custom code developed in MatLab 7 (Mathworks Inc., Natick MA, USA) was used.[28] It consisted of spatial realignment, slice-timing correction and normalization to 2 mm MNI space by co-registration to the individual T1 structural scan and subsequent segmentation and normalization. Manual censoring of movement-affected segments was performed, leading to rejection of one or more volumes in 42 patients (median number of rejected volumes 38). Movement-related variance was removed by multilinear regression, with 3rd order polynomial detrending and 0.1 Hz low-pass filtering. Residual global signal fluctuations were regressed out and 8 mm smoothing was applied.

Independent Component Analysis (ICA)

ICA was performed independently for each participant, using the group ICA of fMRI toolbox (GIFT, MIALab, University of New Mexico, USA) and a fixed number of 20 components [33] which were saved in z-rescaled format. To enable automatic rating of the DMN, the following steps were applied: 1) a DMN mask was derived thresholding a statistical group map (t>5) computed over the control participants, selecting the three posterior nodes (precuneus with extension to posterior cingulate cortex (PCC), and left and right parietal cortex (LPC and RPC)), while the medial frontal cortex (MFC) node was excluded as its activity was weaker in our controls and generally in DOC patients,[27] and thus rendered DMN identification less reliable; 2) for each participant and component (thresholded at z>2), proportion of supra-threshold voxels was calculated separately for the PCC, LPC and RPC and averaged, then the percentage of supra-threshold voxels outside the DMN mask was subtracted from each individual component, and the difference map was thresholded at z>0.20; 3) in case of no supra-threshold components (50%) the DMN map was zero-filled. After DMN identification using the above procedure, to quantify PCC, LPC, RPC and MFC activity (MFC included for measurement, though not relied upon the DMN identification) the proportion of z>2 voxels was measured separately for each region.[34]

Seed-Based Analysis (SBA)

SBA was independently performed for 6 seeds, located in left and right PCC, LPC, RPC, left and right MFC. These were defined based on a pre-existing DMN group map [35] intersected with corresponding AAL atlas cortical regions (67, 68, 65, 66, 23 and 24 [36]). The mean time-course of each seed was entered into a correlation analysis, and corresponding statistical maps were thresholded at t>4. For SBA, no automatic measurements were performed given that in many cases very strong and diffuse, unspecific correlation was observed; hence, for this technique expert

inspection of the maps was essential to determine whether a DMN-related topographical pattern was present or not.

Rs-fMRI Visual Ratings

For each patient, rating was performed by two expert investigators blind to all patient data. The component(s) visualizing DMN activity were manually chosen from the 20 extracted by ICA. Since DMN activity could split over 2 (left and right) ICA components, up to 2 components could be chosen. Overall, 66% of patients had no identifiable DMN, 25% had DMN in one ICA component and 9% had DMN in two ICA components. During selection of the ICA component(s) showing DMN activity, SBA maps were also visualized to increase operator confidence. The DMN was then rated in three different manners during separate sessions. First, considering the ICA map alone and assigning a score of 0 or 1 to each node: for this analysis, all scores were clamped to zero if no DMN component could be identified in the previous step. Second, considering only the 6 SBA maps and assigning a score of 0, 0.5 or 1 to each node: for this analysis, 0.5 was assigned if correlated activity was observed for a given node on one map only, and 1 was assigned if it was visible on two or more maps. Third, considering SBA+ICA together: for this analysis a score of 0.5 was assigned to each node if correlated activity beyond the PCC was visible on ICA and SBA maps. Across all sessions, the operators searched for presence of clear, well-defined clusters of correlated activity resembling the known DMN pattern established on controls; in particular, large clusters of correlated activity, without anatomical specificity, were disregarded.

Ratings were given independently by the two raters, then reconsidered in cases of disagreement; they were thereafter summed across nodes and averaged across the raters, yielding for each patient three overall scores: ICA alone, SBA alone and ICA+SBA together. Inter-rater agreement was 92% for DMN identification, and ρ=0.80 for ICA, ρ=0.94 for SBA and ρ=0.90 for ICA+SBA.

sMRI Visual Rating

Two expert neuroradiologists blind to all patient data rated the severity of gross anatomical and signal abnormality corresponding to the expected DMN nodes location according to the following scale: 0 (severely damaged, i.e. parenchyma obliterated and/or intense, pervasive hyper-intensity), 1 (recognizable but distorted morphology and/or severe signal abnormality), 2 (moderate anatomical damage and/or signal abnormality), 3 (mild anatomical damage and/or signal abnormality) to 4 (normal-appearing). Ratings were given independently by the two raters, and reconsidered in cases of large disagreement; the scores were then averaged together. Inter-rater agreement was ρ=0.88.

FDG-PET Data Acquisition and Analysis

Scanning was performed on a Biograph Truepoint 64 PET/CT scanner (Siemens, Erlagen, DE). Patients rested in a quiet, dimly lit room during FDG uptake (140 MBq±30 MBq) for at least 40 min. Each acquisition included a transmission scan followed by a three-dimensional (3D) static emission for 15 min. PET sections were reconstructed using iterative ordered-subset expectation maximization (6 iterations, 8 subsets), corrected for scatter and attenuation, then reconstructed to in-plane voxel-size 1.3 mm, thickness 3.0 mm.

Standardized uptake value (SUV) maps were derived as SUV=AC/(FDGdose/BW), where AC in kBq/ml represents activity concentration in a given voxel, FDGdose in MBq is the injected radiotracer dose corrected for residual activity in the syringe, and BW in kg is the body weight. SUV maps were thereafter coregistered using SPM12 to individual volumetric T_1-series, which were segmented to generate the normalization deformation field to be applied to the coregistered FDG-PET scan. The normalised PET images were finally smoothed with a 10 mm isotropic Gaussian filter. Using the DMN mask derived from the controls as described above for ICA analysis, the average SUV values for PCC, LPC, RPC and MFC were computed.

Voxel-wise group map analyses

Group-level analyses were performed using Statistical Non-Parametric Mapping (SnPM; http://warwick.ac.uk/snpm) which implements a non-parametric multiple comparisons procedure based on randomisation/permutation.[37] This was chosen as data were not normally distributed due to presence of zero-filled DMN maps. We conducted separate analyses for ICA, SBA (combining the maps from the left and right PCC via voxel-wise maximum) and FDG-PET. For each technique, we performed 1) a correlation analysis with respect to diagnosis encoded as 0: VS/UWS, 1: MCS and 2: SD (after Ref 20), 2) a correlation analysis with respect to the CRS-R score and 3) a group comparison between VS/UWS and MCS.

Statistical analyses

As indicated in Table 1, statistical analyses were performed on four subsamples: 1) all patients (n=119); 2) the 75% of patients with smallest median frame-to-frame displacement as obtained from rigid-body frame realignment (n=89); 3) all patients who underwent FDG-PET (n=85); 4) patients from 2) who also underwent FDG-PET (n=62). This subdivision was necessary due to the uneven number of patients for whom MRI and PET data were available, and to highlight rs-fMRI sensitivity to head movement; the 75% threshold was determined a-priori in preliminary analyses, blinded to the present data. As indicated below, this threshold corresponds to median frame-wise displacement of about 0.3 mm, which is moderately conservative according to the criteria described in Ref [38,39]. This allows us to reject those cases that in other studies would have likely been rejected outright due to excessive movement.

We considered the 'entire DMN' combining scores (i.e. arithmetic averaging) of the MFC, PCC and left and right LPC and, separately, the 'posterior DMN' combining PCC, left and right LPC scores, as correlated activity is weaker in MFC compared to the posterior nodes.

We assessed the statistical association of the imaging modalities (sMRI, rs-fMRI and FDG-PET) with respect to the VS/UWS and MCS diagnosis by means of a logistic regression model. First, univariate logistic models were performed for each predictor i.e. imaging modality ($p<0.05$), then only the significant variables were considered for the development of a multivariate logistic regression model. A backward selection procedure ($p<0.05$) starting with the inclusion of all predictors was used to eliminate non-significant predictors and to identify a final parsimonious multivariate logistic model i.e. which accomplishes the desired level of explanation with as few predictors as possible. From each final multivariate model, the maximum likelihood estimator provided a score for each patient which was used to estimate the area under a "receiver operating characteristics" curve (AUC). AUC was used as measure of diagnostic discrimination for univariate and multivariate logistic models; the equality of correlated AUCs were compared using the Stata's *roccomp* command (Stata Statistical software, 12, College Station, USA)[41].

Furthermore, correlations between the imaging scores and the CRS-R score and between the level of structural damage (sMRI) and the functional modalities (rs-fMRI, FDG-PET) were assessed with non-parametric Spearman's ρ ($p<0.05$). To estimate 95% CI, Fisher's z-transformation and Fisher's bias correction were used. To assess the presence of heterogeneity with respect to aetiology (traumatic, vascular, anoxic) and DMN nodes (PCC, LP, MFC) a Q test was used ($p<0.05$); to quantify the degree of heterogeneity the I^2 index was used[41].

RESULTS

Group analyses

As shown in Suppl Table 1, over the whole sample (*100% of ALL*, n=119), sMRI visual ratings of anatomical damage predicted VS/UWS from MCS and correlated moderately with CRS-R scores (up to $\rho=0.35$). Conversely, none of the rs-fMRI measures were sensitive to diagnosis and

correlations with CRS-R scores were weak (ρ~0.2). Excluding the quartile with largest head movement (*75% of ALL*, n=89), significant prediction between VS/UWS and MCS appeared for almost all rs-fMRI measures, with moderate correlation with the CRS-R score (up to ρ=0.35, see Suppl Table 1). Out of the four rs-fMRI measures considered, visual ratings of SBA and SBA+ICA yielded the strongest results, although all rs-fMRI measures were highly correlated (ρ~0.85). Considering the sub-sample of patients who underwent FDG-PET (*100% of ALL with PET*, n=85), SUV values predicted VS/UWS and MCS, and lead to the highest correlation with the CRS-R score (ρ=0.41); in this sub-sample, sMRI ratings maintained similar performance to the above, but rs-fMRI measures were poorly informative. Excluding the quartile with largest head movement and considering only the sub-sample of patients who underwent FDG-PET (*75% of ALL with PET*, n=62), sMRI and FDG-PET measures slightly diminished. Even if considering all DMN nodes or only posterior regions lead to similar results, correlation and significance scores tended to be stronger for the posterior nodes.

As visualized in Figure 1, voxel-wise statistical analyses suggested that ICA was superior to SBA, showing an effect of diagnosis, and correlation with the CRS-R scores was more clearly localized to the DMN nodes. This result seems at odds with SBA visual ratings which yielded significant results (Suppl Table 1), may be for two reasons: visual ratings are guided by expert heuristics, whereas voxel-wise statistics may be more vulnerable to localization variability, and SBA visual ratings were performed considering maps from all six seeds, whereas voxel-wise group maps were generated considering only the precuneus as seed. As regards FDG-PET, voxel-wise analyses of SUV maps delineated a broader set of regions, which encompass the posterior DMN nodes; while correlation with the CRS-R yielded a clear and broader effect, comparison of MCS vs. VS/UWS lead to a more constrained difference.

Figure 2 shows the diagnostic accuracy of each modality, represented in its "optimal" conditions, following the results reported in Suppl Table 2, namely: *i*) sMRI and FDG-PET are relatively insensitive to head movement, therefore they were assessed on all available cases, *ii)* for sMRI and FDG-PET, results are consistently stronger when only the posterior nodes are considered, therefore the posterior DMN was considered for these techniques, and *iii)* for rs-fMRI, the visual rating of ICA+SBA was chosen as it was the only predictor retained by multivariate logistic regression with backward prediction selection including all four rs-fMRI measures. For rs-fMRI, the entire DMN was considered because the frontal node was clearly involved in the group analyses (Figure 1), though the results were similar for the entire DMN and the posterior DMN. Results show that, while AUCs were modest, FDG-PET lead to the best classification accuracy between VS/UWS and MCS patients (AUC=0.75), followed by sMRI (AUC=0.72) and by rs-fMRI (AUC=0.65). Correlations with CRS-R were moderate ($0.31<\rho<0.41$) and followed a similar pattern. All modalities revealed significant differences between VS/UWS and MCS.

Consideration of the logistic regressions and AUCs for separating VS/UWS and MCS patients (Suppl Table 2) revealed the following. *i*) Over the entire population (*100% of ALL*, n=119), sMRI was significantly superior to rs-fMRI. *ii*) Excluding the quartile with largest head movement (*75% of ALL*, n=89), their performance was similar. *iii*) Considering all patients who underwent FDG-PET (*100% of ALL with PET*, n=85), sMRI and FDG-PET had similar performance and were clearly superior to rs-fMRI. In multivariate logistic regression, sMRI and FDG-PET were retained in the model, but rs-fMRI was eliminated; the performance of the multivariate model was comparable to that of the single predictors (see AUCs). *iv*) Excluding the quartile with largest head movement and considering only the sub-sample of patients who underwent FDG-PET (*75% of ALL with PET*, n=62), sMRI and rs-fMRI provided similar performance, and FDG-PET was slightly superior to both. In multivariate logistic regression, rs-fMRI and FDG-PET were retained in the

model, but sMRI was eliminated; the performance of the multivariate model was comparable to that of the single predictors (see AUCs).

Effect of head movement

Suppl Table 3 shows the proportion of patients in each group (VS/UWS, MCS and SD) for whom DMN activity was detected, empirically defined as a score ≥1 on visual assessment of ICA+SBA, corresponding to detection of correlated activity between at least two DMN nodes. In the entire sample, head movement was largest for the MCS group, and rejection of the top quartile or half with largest head movement had the highest impact on this population (DMN detection ratio increased from 36% to 83%). By contrast, for SD patients the DMN was always detected, and for VS/UWS patients the detection ratio remained relatively stable.

For comparison, head movement was also calculated according to the well-accepted formula described in Ref [39], which includes rotations assuming a mean distance of 50 mm between cerebral cortex and head centre. Across all patients, this measure and the simple median displacement here considered for excluding high-movement cases were almost perfectly correlated (ρ>0.99). The 75th percentile chosen as a threshold corresponded to a median frame-wise displacement of about 0.3 mm, which is moderately conservative according to the criteria described in Ref [39].

Lateralization

Following the asymmetry visible in Figure 1, we conducted additional analyses separately for the left and right hemispheres, aiming to ascertain possible lateralization of predictability of VS/UWS vs. MCS (Suppl Table 4). Overall, left hemispheric integrity was more strongly predictive of clinical status. Specifically, for sMRI and FDG-PET, univariate logistic regressions indicated that left and right hemispheres were both predictive, but multivariate logistic regression retained only

the left. For rs-fMRI, the visual rating of ICA+SBA only provided separate hemispheric scores for the lateral parietal cortex (LPC), and only the left side was significantly predictive. We thus also considered automated ICA rating (proportion of supra-threshold voxels across MFC, PCC and LPC) separately for the two hemispheres; here too, only the left side provided significant results.
As regards to the single DMN regions, for sMRI and rs-fMRI, the AUCs for separating VS/UWS from MCS were generally left-lateralized among the PCC and LPC considered separately and the overall DMN, but lower for the MFC. For FDG-PET, lateralization in the separate DMN regions was overall less evident.

Effect of etiology

In spite of limited numerosity for some patient sub-samples, we calculated separate AUC values for the three etiology groups (traumatic, vascular, anoxic). The Q test and I^2 index did not reveal significant heterogeneity, indicating that the modalities had comparable diagnostic power irrespective of etiology. Nevertheless, for sMRI and rs-fMRI, the AUC was consistently highest for anoxic, followed by traumatic, and then by vascular etiology, across the four sub-samples (Suppl Table 5).
As regards to the relationship between structural damage (sMRI) and results of rs-fMRI, the correspondence was strongest for anoxic etiology closely followed by traumatic etiology, and considerably weaker for vascular etiology; for FDG-PET, the correspondence with sMRI was also strongest for anoxic etiology, but here a graded effect was observed, with weaker correlation for vascular followed by traumatic etiology (Suppl Table 6).

Clinical data as well as automatic and rating data performed on sMRI, rs-fMRI and FDG-PET are reported in Suppl. Table 7.

Two anecdotal cases

Despite the above limitations, rs-fMRI may provide important additional information complementing the other modalities for some cases. Among patients clinically diagnosed in VS/UWS, 7 out of 72 had a score ≥2 for ICA+SBA visual rating, indicating high DMN preservation. Out of these, two are described in detail to exemplify cases where the other techniques do not provide conclusive results, but the presence of a near normal-appearing DMN could indicate residual brain activity, motivating enhanced rehabilitation efforts. As limited follow-up data are available, this is only reported as anecdotal evidence. Of the remaining patients, 4 had remained stable and 1 had slightly deteriorated two years after scanning.

Case 1 (55-year-old woman, alias VS/UWS_24 in Suppl. Table 7) suffered a ruptured aneurysm, had disease duration 23 months and CRS-R score 6. Severe fronto-parietal infarction, superficial siderosis and left-sided atrophy were evident at MRI. FDG-PET identified a markedly asymmetrical pattern, with severe left hemisphere hypometabolism and relative right hemisphere preservation. EEG was markedly asymmetric, with slowed and reduced amplitude activity on the left and predominant theta activity on the right, and auditory cognitive evoked potentials (auditory P300; auditory mismatch negativity, MMN) were present. Rs-fMRI revealed a clear pattern of correlated activity in DMN nodes. The integrity of functional connections among bilateral precuneus, medial frontal cortex and right lateral parietal cortex was concordantly confirmed by ICA and SBA; by contrast, synchronized activity in the left lateral parietal cortex was never detected, even when this area was considered as SBA seed. Two years after scanning, the CRS-R visual scale improved for presence of visual pursuit, and diagnosis was changed to MCS.

Case 2 (76-year-old man, alias VS/UWS_66 in Suppl. Table 7) suffered post-surgical brain haemorrhage, had disease duration 15 months and CRS-R score 6. Severe bilateral frontal atrophy,

white matter hyperintensity and superficial siderosis were evident at MRI. FDG-PET identified severe hypometabolism in the right frontal area and moderate left fronto-parietal hypometabolism. Symmetric EEG with slowed and reduced amplitude activity and localized interictal epileptiform activity were present, and auditory cognitive evoked potentials (P300, MMN) were absent. Rs-fMRI revealed correlated activity in all posterior DMN regions and this pattern was more evident with SBA than ICA. As regards to the medial frontal node, no correlated activity was detected; when considering this area as seed region, spurious clusters of correlated signal appeared in the fornix and ventricles, plausibly due to the non-neural physiological signal fluctuations often observed in these regions. In conjunction with a treatment of amantadine, the patient improved for the presence of visual pursuit and was diagnosed as MCS for approximately one year.

DISCUSSION

We investigated the integrity of DMN in relation to consciousness with rs-fMRI in the largest group of DOC patients studied so far, directly comparing rs-fMRI with sMRI and PET. We confirm a significant relationship between functional, anatomical and metabolic integrity of the DMN and clinical status, and provide additional insight on the potential clinical contribution of each technique.

Rs-fMRI analyses and their sensitivity to clinical status

Our data show that DMN functional connectivity strength differentiates MCS from VS/UWS patients, correlating with the clinical status measured with CRS-R, in line with other studies.[20] Excluding patients with largest head movement, all four rs-fMRI measures (auto ICA, visual ICA, visual SBA visual ICA+SBA) indicated that greater correlated activity within the DMN was

associated to higher consciousness level. While ICA-SBA agreement is overall good, visual ratings of SBA alone and SBA+ICA together yielded the strongest statistical scores because considering multiple maps allowed more confident and reliable assessment. We therefore advise that, when possible, ICA and SBA should be combined or multiple SBA seeds should be considered. Notably, automatic and visual rating yielded similar results, reassuring that implementing in clinical routine rs-fMRI based on expert visual assessment is acceptable, even though automated rating can be less biased.

In our study the DMN was identifiable in ~30% of VS/UWS cases and in ~59% of MCS cases, ranging from 36% to 83% depending on the number of patients excluded for head movement, and always recognizable in SD cases. However, attention was focused on VS/UWS to determine whether patients show residual functional activity and sign of consciousness. For cases where diagnostic classification is uncertain, evidence of synchronized activity between anatomically distant nodes could prompt more careful evaluation of the patient's condition.

Limited overall diagnostic accuracy with potential relevance for some individual cases

The results of this study warn about the impact of movement during rs-fMRI. In the favorable scenario of low or no movement, rs-fMRI seems to have high sensitivity to DMN activity; however a sizable proportion of cases, especially MCS patients, move during scanning (Suppl Table 3), curtailing the diagnostic potential of this technique. Indeed, it is customary in studies in this area to focus on patients with acceptably low head movement, rejecting outright cases where acquisitions cannot be performed satisfactorily due to movement. Here, in order to accurately represent the clinical reality, we chose to include all patients that could be scanned and a-posteriori, blinded to the clinical data, we removed those most affected by movement. The overall diagnostic accuracy of rs-fMRI is below accepted thresholds for consideration as a biomarker (AUC=0.65). Univariate and

multivariate regression indicated that sMRI and rs-fMRI had comparable diagnostic accuracy, and that the latter did not provide additional information. Nevertheless, rs-fMRI could yield clinically-impacting results for some individual cases in which the VS diagnosis is uncertain. In a minority of VS/UWS cases of our cohort, this network was clearly identifiable in spite of mediocre or inconclusive results from other modalities. In particular, two cases reported in Fig. 3 emerged from vegetative state in the months following scanning, suggesting that rs-fMRI evidence of preserved synchronized activity may have some prognostic value. This view is supported by a recent study which showed that the level of preservation of fronto-parietal connectivity can predict the clinical outcome of comatose patients at 3 months[24]. We hypothesize that rs-fMRI might be useful for detecting cases where additional diagnostics or increased rehabilitation efforts may be motivated in light of possible conversion to MCS. This question, however, can only be answered via a follow-up study. In our cohort of patients evidence of association between DMN integrity and clinical recovery was limited to two anecdotal cases, and the recovery was quantitatively small, i.e. evolution to MCS was only determined by presence of visual pursuit. Here, only relatively small changes in clinical status could be expected given the long average disease duration of this cohort. DMN integrity is neither a pre-requisite for, nor a direct sign of consciousness,[18,22] nevertheless this network represents a fundamental property of brain function whose relationship to consciousness has repeatedly emerged under diverse conditions.[1]

While fMRI of active imagery tasks such as playing tennis has low sensitivity due to cognitive and compliance demands,[11] its high specificity can have a profound impact on clinical decisions in specific cases.[42,43] In respect to this approach, rs-fMRI of the DMN represents a more indirect assessment of consciousness, but plausibly has significantly higher sensitivity since it does not require any active cognitive capability and for this reason can be employed with all DOC patients. In patients without a clear behavioural response, in particular those deemed to be in VS/UWS,

detection of residual DMN activity by rs-fMRI (which generally requires low head movement level) may prompt more careful evaluation of the patient's condition and of the results given by structural and metabolic imaging.

Relationship to structural and metabolic integrity

Compared to functional measures, the role of conventional structural imaging in the diagnostic work-up of DOC patients has been less thoroughly investigated. In our cohort, expert assessment of gross anatomical changes and signal abnormalities in DMN conveyed information useful for differentiating VS/UWS and MCS patients at group level (Suppl Table 1). Although structural integrity of the DMN alone cannot replace functional and metabolic measures, anatomical damage could deserve more systematic consideration, as recently suggested for critically-ill patients with primary non-neurological disease[44]. This is relevant because structural assessment was far less sensitive to head movement than rs-fMRI, yielding AUC=0.72 over the entire cohort; in addition, a more detailed assessment than the "lumped" damage ranging from 0 to 4 considered here may provide even higher diagnostic accuracy. The importance of assessing structural integrity is further underlined by recent DTI results demonstrating correlation between white matter damage in DMN regions and thalamus, and the level of consciousness.[45]

FDG-PET yielded the best diagnostic accuracy (AUC=0.75) and correlation with CRS-R scores (Fig. 2 and Suppl Table 2), and is less sensitive to head movement, since it has a smoothing effect which is partially masked by the inherent blurring already present ab-initio in the PET images. These results agree with previous studies showing strongest metabolic reduction in the fronto-parietal cortex, [2,10] and confirm that FDG-PET can robustly differentiate MCS from VS/UWS patients at group level.[11,12] Compared to the AUC=0.87 reported in Ref. 12, lower accuracy here is probably ascribable to differences in chosen measurement areas, lesion pattern, etiology and uptake

normalization approach. FDG-PET surpasses rs-fMRI only when all cases are included (N=119), while does not differ significantly when excluding cases most affected by movement (N=89, Suppl Table 2). Compared to rs-fMRI, FDG-PET provides a global measure of brain metabolism, which is less functionally specific than assessment of residual synchronization in the DMN network. As such, the two techniques should be considered complementary and not competing.

Importantly, excluding the patients with largest head movement, sMRI, rs-fMRI and PET did not differ significantly and the performance of a multivariate model including two modalities was only slightly superior to that of the single modalities. Overall, there is no evidence that one technique is significantly superior to the other.

Based on behavioural observation of patients undergoing the Wada test (amobarbital injection), it has been hypothesized that functional preservation of left hemispheric function has greater impact on level of consciousness than right hemispheric function (e.g. Ref [46-48]). However a large-scale study of patients with acute hemispheric stroke found no statistically-significant evidence of lateralization[49]. Thus, evidence for left-lateralization of the neural underpinnings of consciousness remains controversial. This issue is important also because DOC patients often have a lateralized damage[50]. Here, we found that differences between VS/UWS vs. MCS patients were stronger for the left than the right hemisphere for all three imaging modalities and that the integrity of the left hemisphere is predictive of a better clinical status. Further confirmation of this finding is required, particularly in a cohort of patients with shorter disease duration, for whom a more univocal cause-effect relationship can be ascertained.

Two important issues not consistently investigated yet are the effects of disease duration and etiology. Most of rs-fMRI studies have been conducted on patients on average in sub-acute phase

(~6-12 months [20,21,23,29]). Our cohort had a substantially longer disease duration (25 months for VS/UWS and 40 months for MCS on average), closer to FDG-PET work (~24 months, or more [12]). Our data extend previous rs-fMRI data showing that a clear relationship between the integrity of DMN activity and clinical status is also found in chronic patients. This result is important because following the initial injury, multiple pathophysiological processes ensue, such as inflammation, secondary degeneration and plastic re-organization, which may diversely impact DMN activity. We found no evidence for preferential diagnostic utility of the three modalities as a function of etiology: this could also be related to the small size of the subsamples, as well as to the multitude of factors associated with the long disease duration in this cohort. Anyhow, our results suggest that the distinction between SV and MCS is easier for the anoxic etiology based on both sMRI and rs-fMRI modalities, probably because anatomical damage tends to be more widespread and consistently severe for these cases, similarly impacting anatomy and function. The SV-MCS distinction is more difficult for vascular (ischaemic and hemorragic) etiology probably because in these cases there is more nuanced and heterogeneous damage to the cortex and white matter, engendering anatomy-function dissociations and making it difficult to objectively assess damage.

Study limitations

The unavailability of FDG-PET for some patients, together with the need to exclude rs-fMRI scans most severely affected by head movement, determined a split into four sub-populations, complicating the comparability of techniques. This limitation was addressed by choosing the best situation for each modality, and importantly the main conclusions were supported by similar results across subpopulations. Follow-up clinical data were only sparingly available and prognostic analyses thus were not performed. We did not consider the effect of thalamic integrity, as this

structure was not consistently observed in DMN maps even for control participants, in line with previous studies.[51,52]

Recent advances in rs-fMRI methodology may increase diagnostic accuracy compared to the methods used here. Multi-band techniques yield longer-time series (>1,000 frame) for the same acquisition time resulting in a drastic improvement of statistical power.[53] Within-frame motion correction, vision-guided prospective motion correction and multi-echo imaging may significantly reduce sensitivity to head movement.[54,55] Additional improvement may be attainable including temporal derivatives, regressor temporal filtering, cardiac and respiratory regressors.[56]

Finally, it should be noted that not even the CRS-R scale is a gold-standard quantification of the patient's clinical condition, because scores partially overlap between different diagnoses and because it embodies the assumption that if a patient is able to show higher-level behaviors then also lower-level responses should be preserved. Future neuroimaging studies may consider revised versions of this scale that attempt to address these issues[57].

CONCLUSIONS

In summary, we confirm that rs-fMRI can be informative about DMN integrity in DOC patients, yielding modest but clearly significant correlation with clinical status. The viability of this technique is critically dependent on head movement, whereas structural MRI and FDG-PET are much less affected. Structural integrity across DMN regions also correlates with consciousness level and FDG-PET yields the highest accuracy scores. Multiple rs-fMRI analyses provided convergent results, and on the whole rs-fMRI does not significantly add to structural MRI and FDG-PET. Nevertheless, so long as patients with largest head movement are excluded, there is also no evidence that either of these techniques is superior to rs-fMRI. Furthermore, all modalities provided tentative evidence that DMN integrity in the left hemisphere may be more predictive of clinical status than the right hemisphere. In patients without a clear behavioural response, rs-fMRI

could be useful in the clinical routine to complement existing diagnostic tools, to detect residual brain activity in individual cases, particularly when results from the other techniques are inconclusive.

ACKNOWLEDGMENTS

The Coma Research Centre (CRC) project was funded by a healthcare grant from the Lombardia regional government (Grant No. IX/000407 - 05/08/2010).

The Coma Research Centre (CRC), on behalf of which the present publication was submitted, acknowledges the following members: Andronache A, Benti R, Bruzzone MG, Caldiroli D, Ciaraffa F, Covelli V, D'Incerti L, Fazio P, Ferraro S, Franceschetti S, Giovannetti A, Leonardi M, Marotta G, Minati L, Molteni F, Nigri A, Pagani M, Panzica F, Parati EA, Reggiori B, Rosazza C, Rossi D, Sattin D, Varotto G, Vela Gomez J.

The study was conducted in collaboration with the European Biomedical Research Federation (FERB).

The authors would like to thank two anonymous reviewers for insightful advice on an earlier version of the manuscript.

AUTHOR CONTRIBUTION

CR AA ML LDI LM were involved in study concept and design.

CR AA DS MGB GM AN SF DRS LP AB RB ML LDI LM acquired and analyzed the data.

CR GM LDI LM drafted the manuscript.

LDI and LM contributed equally to this article.

CONFLICTS OF INTEREST

On behalf of all authors, the corresponding author states that there is no conflict of interest.

REFERENCES

1. Giacino JT, Fins JJ, Laureys S, Schiff ND. Disorders of consciousness after acquired brain injury: the state of the science. Nat Rev Neurol. 2014;10:99-114.

2. Laureys S, Owen AM, Schiff ND. Brain function in coma, vegetative state, and related disorders. Lancet Neurol. 2004;3:537-46.

3. Owen AM1, Coleman MR. Functional neuroimaging of the vegetative state. Nat Rev Neurosci. 2008;9:235-43.

4. Casali AG, Gosseries O, Rosanova M, Boly M, et al. A theoretically based index of consciousness independent of sensory processing and behavior. Sci Transl Med. 2013;5(198)

5. Leonardi M, Sattin D, Raggi A. An Italian population study on 600 persons in vegetative state and minimally conscious state. Brain Inj. 2013;27:473-84.

6. Hannawi Y, Lindquist MA, Caffo BS, Sair HI, et al. Resting brain activity in disorders of consciousness: a systematic review and meta-analysis. Neurology. 2015;84:1272-80.

7. Fernández-Espejo D, Bekinschtein T, Monti MM, Pickard JD, et al. Diffusion weighted imaging distinguishes the vegetative state from the minimally conscious state. Neuroimage. 2011;54:103-12.

8. Levy DE1, Sidtis JJ, Rottenberg DA, Jarden JO, et al. Differences in cerebral blood flow and glucose utilization in vegetative versus locked-in patients. Ann Neurol. 1987;22:673-82.

9. Laureys S, Schiff ND. Coma and consciousness: paradigms (re)framed by neuroimaging.

Neuroimage. 2012;61:478-91.

10. Laureys S, Goldman S, Phillips C, Van Bogaert P, et al. Impaired effective cortical connectivity in vegetative state: preliminary investigation using PET. Neuroimage. 1999;9:377-82.

11. Stender J, Gosseries O, Bruno MA, Charland-Verville V, et al. Diagnostic precision of PET imaging and functional MRI in disorders of consciousness: a clinical validation study. Lancet. 2014;384:514-22.

12. Stender J, Kupers R, Rodell A, Thibaut A, et al. Quantitative rates of brain glucose metabolism distinguish minimally conscious from vegetative state patients. J Cereb Blood Flow Metab. 2015;35:58-65.

13. Raichle ME, MacLeod AM, Snyder AZ, Powers WJ, et al. A default mode of brain function. Proc Natl Acad Sci U S A. 2001;98:676-82.

14. Greicius MD1, Krasnow B, Reiss AL, Menon V. Functional connectivity in the resting brain: a network analysis of the default mode hypothesis. Proc Natl Acad Sci U S A. 2003;100:253-8.

15. Buckner RL, Andrews-Hanna JR, Schacter DL. The brain's default network: anatomy, function, and relevance to disease. Ann N Y Acad Sci. 2008;1124:1-38.

16. Fox MD, Raichle ME. Spontaneous fluctuations in brain activity observed with functional magnetic resonance imaging. Nat Rev Neurosci. 2007;8:700-11.

17. Rosazza C, Minati L. Resting-state brain networks: literature review and clinical applications. Neurol Sci. 2011;32:773-85.

18. Boly M, Tshibanda L, Vanhaudenhuyse A, Noirhomme Q, et al. Functional connectivity in the default network during resting state is preserved in a vegetative but not in a brain dead patient. Hum Brain Mapp 2009;30:2393–2400.

19. Cauda F, Micon BM, Sacco K, Duca S et al. Disrupted intrinsic functional connectivity in the vegetative state. J Neurol Neurosurg Psychiatry 2009;80:429–431.

20. Vanhaudenhuyse A, Noirhomme Q, Tshibanda LJF, et al. Default network connectivity reflects the level of consciousness in noncommunicative brain-damaged patients. Brain 2010;133:161–171.
21. Crone JS, Ladurner G, Höller Y, Golaszewski S, et al. Deactivation of the default mode network as a marker of impaired consciousness: an fMRI study. PLoS One. 2011;6:e26373.
22. Norton L, Hutchison RM, Young GB, Lee DH, et al. Disruptions of functional connectivity in the default mode network of comatose patients. Neurology. 2012;78:175-81.
23. Di Perri C, Bastianello S, Bartsch AJ, Pistarini C, et al. Limbic hyperconnectivity in the vegetative state. Neurology. 2013;81:1417-24.
24. Silva S, de Pasquale F, Vuillaume C, Riu B, et al. Disruption of posteromedial large-scale neural communication predicts recovery from coma. Neurology. 2015;85:2036-44.
25. Wee CY, Yap PT, Zhang D, Denny K, et al. Identification of MCI individuals using structural and functional connectivity networks. Neuroimage. 2012;59:2045-56.
26. Dai Z, Yan C, Wang Z, Wang J, et al. Discriminative analysis of early Alzheimer's disease using multi-modal imaging and multi-level characterization with multi-classifier (M3). Neuroimage. 2012;59:2187-95.
27. Qi R, Zhang LJ, Luo S, Ke J, et al. Default mode network functional connectivity: a promising biomarker for diagnosing minimal hepatic encephalopathy: CONSORT-compliant article. Medicine (Baltimore). 2014;93:e227.
28. Andronache A, Rosazza C, Sattin D, Leonardi M, D'Incerti L, Minati L; Coma Research Centre (CRC) – Besta Institute. Impact of functional MRI data preprocessing pipeline on default-mode network detectability in patients with disorders of consciousness. Front Neuroinform. 2013;22:7-16.
29. Demertzi A, Gómez F, Crone JS, Vanhaudenhuyse A, et al. Multiple fMRI system-level baseline connectivity is disrupted in patients with consciousness alterations. Cortex. 2014;52:35-46.
30. Giacino JT. Disorders of consciousness: differential diagnosis and neuropathologic features. Semin Neurol. 1997;17:105-11.

31. Giacino, J. T., Kalmar, K., & Whyte, J. The JFK Coma Recovery Scale-Revised: measurement characteristics and diagnostic utility. Archives of Physical Medicine and Rehabilitation, 2004;85(12), 2020e2029.

32. Lombardi F, Gatta G, Sacco S, Muratori A, Carolei A. The Italian version of the Coma Recovery Scale-Revised (CRS-R). Funct Neurol. 2007;22:47-61.

33. Calhoun VD, Adali T, Pearlson GD, Pekar JJ. A method for making group inferences from functional MRI data using independent component analysis. Hum Brain Mapp 2001;14:140–151.

34. Tie Y, Rigolo L, Norton IH, Huang RY, Wu W, Orringer D, Mukundan S Jr, Golby AJ. Defining language networks from resting-state fMRI for surgical planning--a feasibility study. Hum Brain Mapp. 2014 35(3):1018-30.

35. Rosazza C, Minati L, Ghielmetti F, Mandelli ML, et al. Functional connectivity during resting-state functional MR imaging: study of the correspondence between independent component analysis and region-of-interest-based methods. AJNR Am J Neuroradiol. 2012; 33:180-7

36. Tzourio-Mazoyer N, Landeau B, Papathanassiou D, Crivello S et al. Automated anatomical labeling of activations in SPM using a macroscopic anatomical parcellation of the MNI MRI single-subject brain. Neuroimage 2002;15:273–89.

37. Nichols TE, Holmes AP. Nonparametric permutation tests for functional neuroimaging: a primer with examples. Hum Brain Mapp. 2002;15:1-25.

38. Power JD, Barnes KA, Snyder AZ, Schlaggar BL, Petersen SE. Spurious but systematic correlations in functional connectivity MRI networks arise from subject motion. Neuroimage. 2012;59:2142-54.

39. Power JD1, Mitra A, Laumann TO, Snyder AZ, et al. Methods to detect, characterize, and remove motion artifact in resting state fMRI. Neuroimage. 2014;84:320-41.

40. DeLong ER, DeLong DM, and Clarke-Pearson DL. Comparing the areas under two or more correlated receiver operating characteristic curves: A nonparametric approach. Biometrics 1988;44: 837–845.

41. Higgins JP T & Thompson SG. Quantifying heterogeneity in a meta-analysis. Statistics in Medicine. 2002;21:1539-1558.

42. Owen AM, Coleman MR, Boly M, Davis MH, et al. Detecting awareness in the vegetative state. Science. 2006;313(5792):1402.

43. Monti MM, Vanhaudenhuyse A, Coleman MR, Boly M, et al. Willful modulation of brain activity in disorders of consciousness. N Engl J Med. 2010;362:579-89.

44. Sutter R, Chalela JA, Leigh R, Kaplan PW, et al. Significance of Parenchymal Brain Damage in Patients with Critical Illness. Neurocrit Care. 2015

45. Fernández-Espejo D, Soddu A, Cruse D, Palacios EM, et al. A role for the default mode network in the bases of disorders of consciousness. Ann Neurol. 2012;72:335-43.

46. Serafetinides EA, Hoare RD, Driver M. Intracarotid sodium amylobarbitone and cerebral dominance for speech and consciousness. Brain. 1965;88:107-30.

47. Glosser G, Cole LC, Deutsch GK, et al. Hemispheric asymmetries in arousal affect outcome of the intracarotid amobarbital test. Neurology 1999;52:1583–90.

48. Meador KJ, Loring DW, Lee GP, et al. Level of consciousness and memory during the intracarotid sodium amobarbital procedure. Brain Cogn 1997;33:178–88.

49. Cucchiara B, Kasner SE, Wolk DA, Lyden PD, et al. Lack of hemispheric dominance for consciousness in acute ischaemic stroke. J Neurol Neurosurg Psychiatry. 2003;74:889-92.

50 Bruno MA, Fernández-Espejo D, Lehembre R, Tshibanda L, et al. Multimodal neuroimaging in patients with disorders of consciousness showing "functional hemispherectomy". Prog Brain Res. 2011;193:323-33.

51. Allen EA, Erhardt EB, Damaraju E, Gruner W, et al. A baseline for the multivariate comparison of resting-state networks. Front Syst Neurosci. 2011;5:2.

52. Van Dijk KR1, Hedden T, Venkataraman A, Evans KC, et al. Intrinsic functional connectivity as a tool for human connectomics: theory, properties, and optimization. J Neurophysiol. 2010;103:297-321.

53. Smith SM, Beckmann CF, Andersson J, Auerbach EJ et al. Resting-state fMRI in the Human Connectome Project. Neuroimage. 2013;80:144-68.

54. Todd N, Josephs O, Callaghan MF, Lutti A, et al. Prospective motion correction of 3D echo-planar imaging data for functional MRI using optical tracking. Neuroimage. 2015;113:1-12.

55. Kundu P, Brenowitz ND, Voon V, Worbe Y et al. Integrated strategy for improving functional connectivity mapping using multiecho fMRI. Proc Natl Acad Sci U S A;110:16187-92

56. Beall EB, Lowe MJ. Isolating physiologic noise sources with independently determined spatial measures. Neuroimage. 2007;37:1286-300.

57. Sattin D, Minati L, Rossi D, Covelli V, et al. The Coma Recovery Scale Modified Score: a new scoring system for the Coma Recovery Scale-revised for assessment of patients with disorders of consciousness. Int J Rehabil Res. 2015;38:350-6.

FIGURE

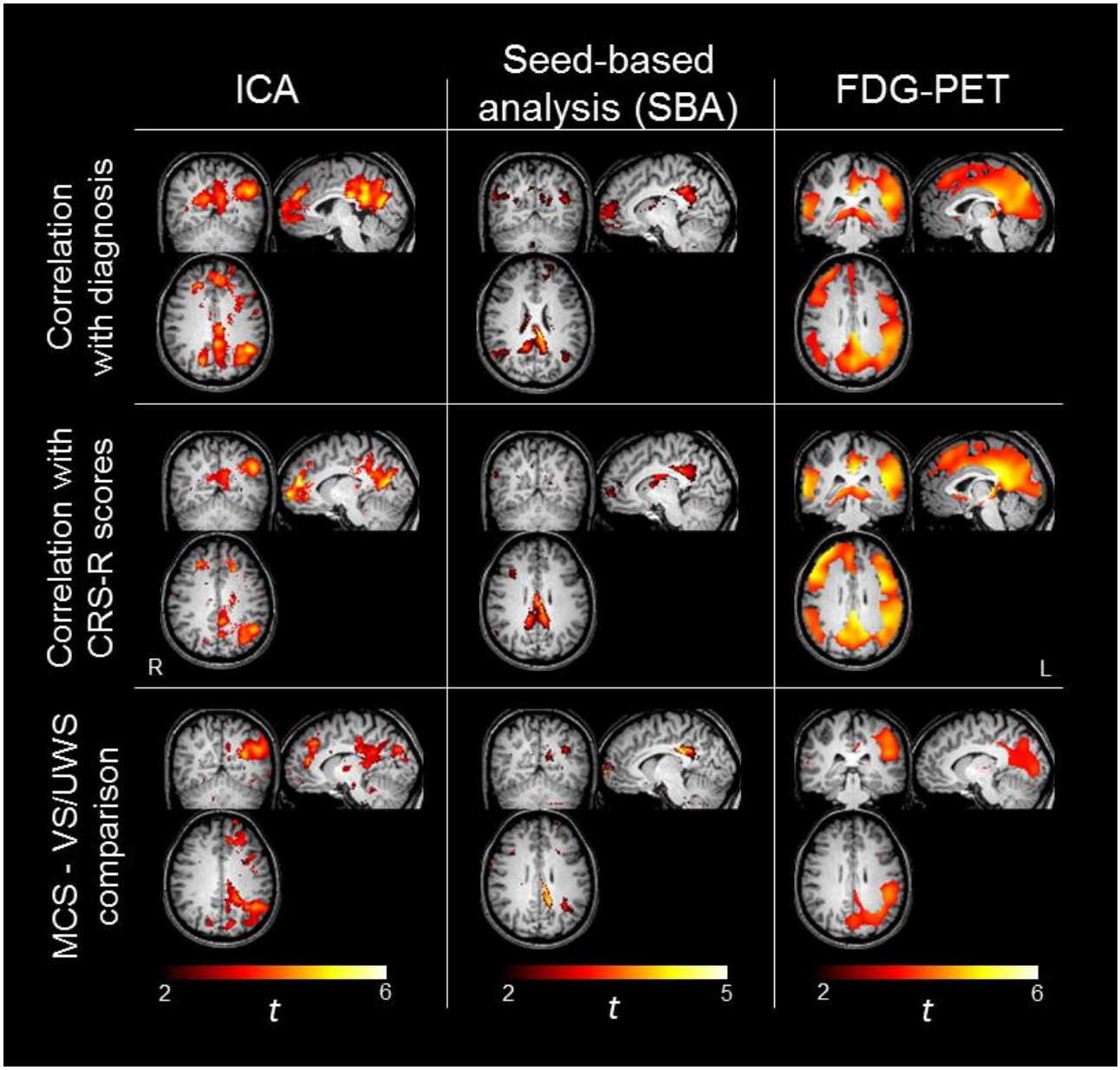

Figure 1. The integrity of the DMN, assessed with rs-fMRI through Independent-component analysis (ICA) and Seed-based analysis (SBA), and additionally with FDG-PET, correlates with clinically-established level of consciousness. A left-lateralized pattern is observed. Analyses were performed on 75% of ALL (n=89) for rs-fMRI data, and on 100% of ALL with FDG-PET (n=85) for FDG-PET data.

Top row: Non-parametric correlation with diagnosis, discretely encoded as vegetative state/unresponsive wakefulness syndrome (VS/UWS), minimally conscious state (MCS), severe disability (SD).

Middle row: Non-parametric correlation with CRS-R scores.

Bottom row: Pair-wise comparison of MCS vs. VS/UWS.

For display purposes, effects are thresholded voxel-wise at P(uncorrected)<0.005 for ICA, P(uncorrected)<0.05 for SBA, and at P(FWE)<0.05 for FDG-PET, and rendered on a canonical T1 brain volume.

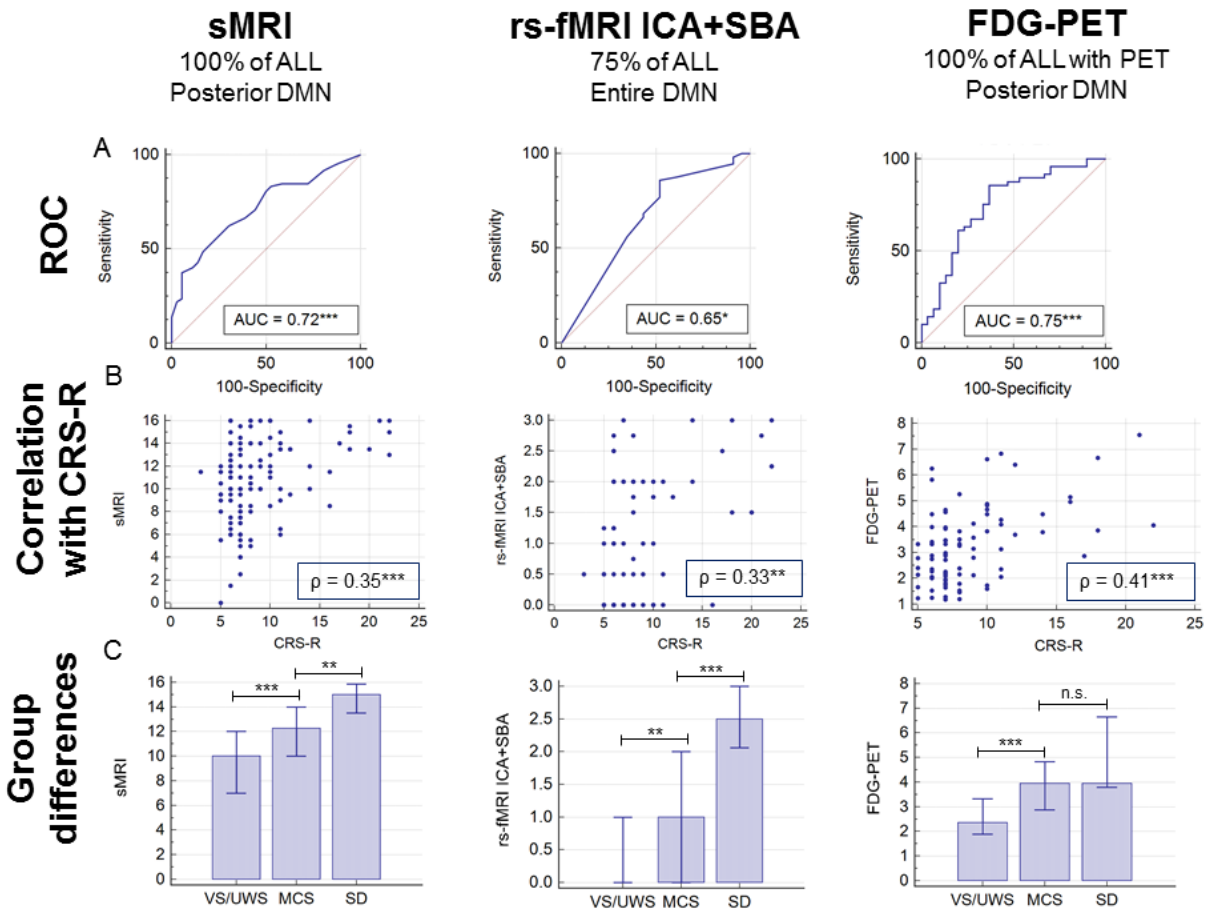

Figure 2. Diagnostic accuracy of sMRI, rs-fMRI and FDG-PET.

A. ROC curves and corresponding area-under-curve (AUC) highlighting significant differences between MCS and VS/UWS.

B. Scatterplot of correlation with CRS-R (Spearman rank-order ρ, over VS, MCS and SD patients).

C. Group differences between VS/UWS, MCS and SD patients (Medians with interquartile range are reported, with Mann-Whitney Z scores). Superscript '*': p<0.05; '**': p<0.01; '***': p<0.001

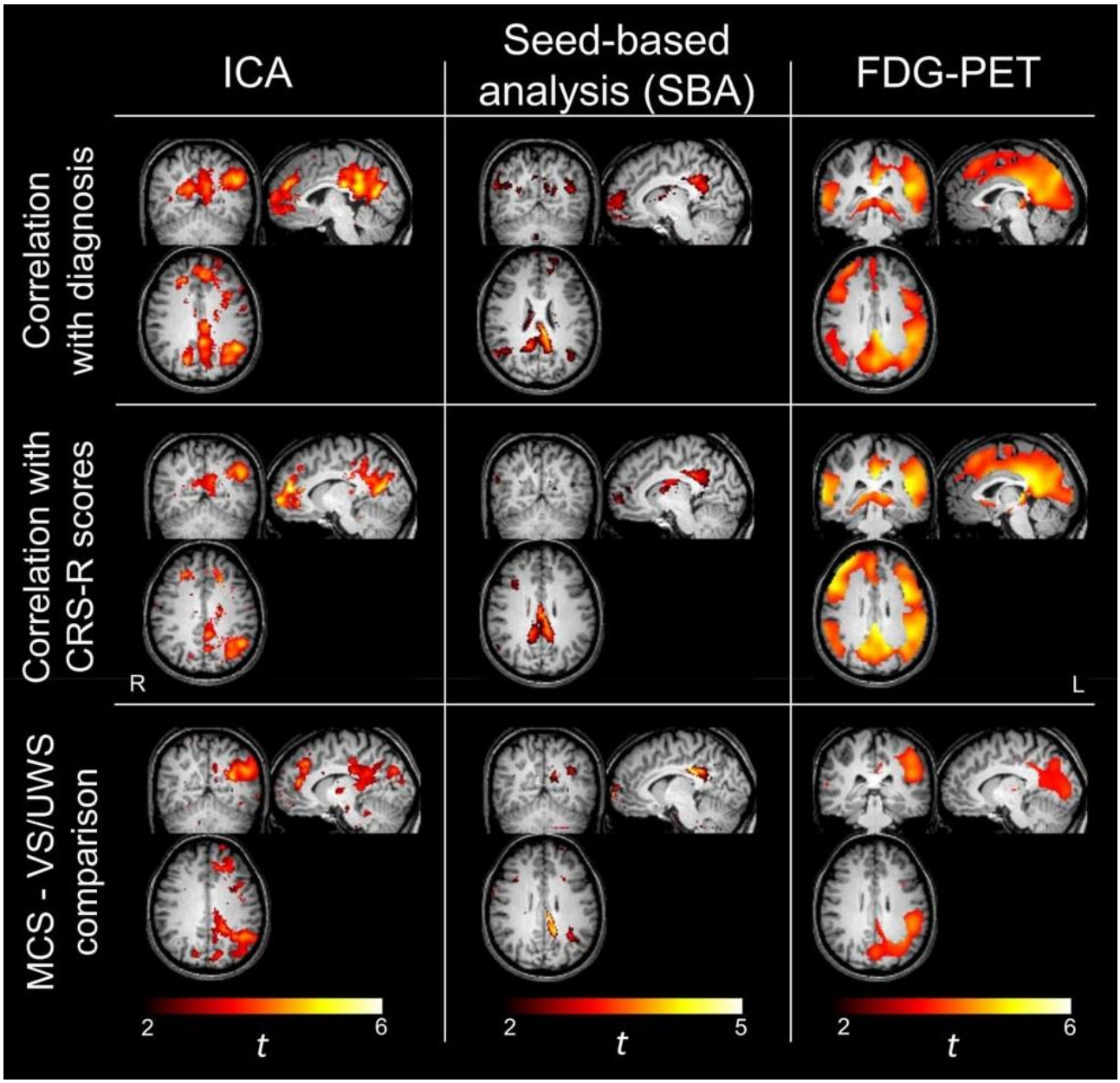

Figure 3. Two patients clinically diagnosed VS/UWS, studied with rs-fMRI, who show complete, near normal-appearing DMN, in spite of inconclusive results from other techniques. Both patients emerged from VS/UWS to MCS in the months after scanning. Although the presence of DMN does not ensure consciousness, its functional integrity may have relevant clinical implications.

For both cases, the DMN was observed with ICA and Seed-Based Analysis (SBA), performed independently for 6 seeds (precuneus extending to the posterior cingulate cortex (PCC), medial frontal cortex (MFC) and lateral parietal cortex (LPC), bilaterally).

For Case 1 (disease duration 23 months, vascular etiology, CRS score 6) DMN activity was consistently detected for all nodes, except for the left LPC, even when this area was considered as SBA seed. For Case 2 (disease duration 15 months, vascular etiology, CRS score 6), the posterior DMN was apparent and this pattern was more evident with ICA than with SBA. Correlated activity was never detected in the MFC; when this area was considered as seed region, spurious non-neuronal clusters were observed. Both cases shows a visible discrepancy between the significant structural damage and the apparently well-preserved DMN activity.

	N	Etiology	Age	Sex (M/F)	Disease duration	CRS-R
100% of ALL	119	36/41/42	52 (19-83)	71/48	26 (2-252)	7 (3-22)
VS/USW	72	19/18/35	52 (21-79)	48/24	26 (3-252)	6 (3-8)
MCS	36	13/18/5	47 (21-83)	16/20	40 (7-209)	10 (7-16)
SD	11	4/5/2	54 (19-67)	7/4	12 (2-41)	18 (14-22)
75% of ALL	89	25/31/33	54 (19-83)	53/36	26 (2-209)	7 (3-22)
VS/UWS	57	13/16/28	55 (21-79)	39/18	26 (3-146)	6 (3-8)
MCS	23	9/10/4	47 (21-83)	9/14	46 (7-209)	9 (7-16)
SD	9	3/5/1	54 (19-67)	5/4	9 (2-41)	20 (14-22)
100% of ALL with PET	85	26/31/28	52 (19-83)	47/38	30 (3-252)	7 (5-22)
VS/UWS	49	12/14/23	52 (21-79)	30/19	25 (5-252)	7 (5-8)
MCS	30	12/15/3	47 (21-83)	13/17	40 (7-209)	10 (7-16)
SD	6	2/2/2	52 (19-66)	4/2	14 (3-31)	18 (14-22)
75% of ALL with PET	62	18/22/22	53 (19-83)	34/28	30 (3-209)	7 (5-22)
VS/UWS	39	8/12/19	53 (21-79)	25/14	26 (5-146)	6 (5-8)
MCS	18	8/8/2	52 (21-83)	6/12	42 (7-209)	10 (7-16)
SD	5	2/2/1	50 (19-60)	3/2	12 (3-31)	18 (14-22)

Table 1. Summary demographic and clinical data. VS/UWS: Vegetative state/unresponsive wakefulness syndrome; MCS: Minimally-conscious state; SD: Severe disability. Etiology is reported as traumatic / vascular / anoxic (N). Age (in years), Disease duration (in months) and CRS-R scores are given as median (range). 75% denotes the subgroup corresponding to exclusion of the quartile with largest head movement during rsfMRI scanning; "with PET" denotes the subgroups of patients for whom FDG-PET data were available.